Available online at www.sciencedirect.com

SciVerse ScienceDirect

Energy Procedia 37 (2013) 5290 – 5297

Energy Procedia

GHGT-11

CO_2 Leakage Prevention by Introducing Engineered Nanoparticles to the In-situ Brine

B. Aminzadeh[a*], D. H. Chung[a], S. L. Bryant[a], C. Huh[a], and D. A. DiCarlo[a]

Department of Petroleum and Geosystems Engineering, The University of Texas at Austin, 1 University Station C0300, Austin, TX 78712, USA

Abstract

Introducing engineered nanoparticles into an aquifer or reservoir can potentially increase the storage efficiency and mitigate the risk of leakage of stored CO_2. We have measured flow pattern and pressure drop during core floods in which high pressure liquid CO_2 or a CO_2 analogue fluid displaces an aqueous suspension of nanoparticles. The displacement front is more spatially uniform and travels more slowly compared to a control displacement with no in-situ nanoparticles. Pressure measurements are consistent with generation of a viscous phase such as an emulsion during the displacement. These observations suggest that a nanoparticle stabilized emulsion is formed during the displacement which acts to suppress the viscous instability.

Selection and/or peer-review under responsibility of GHGT

CO_2 storage, Nanoparticle, Lekage prevention, Mobility control, Emulsion formation

1. Introduction

Carbon capture, utilization, and storage (CCUS) can play an important role in reducing the growing threat of global warming [1]. However, implementing CCUS requires capturing and storing of order a billion metric tons of CO_2 annually [2]. To ensure this large amount is stored securely in depleted reservoirs and/or deep saline aquifers, the long term fate of CO_2 needs to be studied. Typically, CO_2 trapping in a geologic strata is categorized by a) dissolution of CO_2 in brine phase, also known as dissolution trapping, b) residual trapping, where CO_2 is trapped as disconnected blobs because of the capillary pressure, and c) mineralization, where CO_2 reacts with calcium and magnesium and precipitates on the rock surfaces. Large scale storage by these mechanisms carries a negligible risk of leakage over a geologically significant time frame [3]. Structural trapping (trapping of CO_2 as a bulk phase beneath the caprock), however, introduces some uncertainty about the long term fate of CO_2. This phenomenon constitutes a key concern for CO_2 storage in subsurface saline aquifers, as CO_2 is less dense and less

1876-6102
Selection and/or peer-review under responsibility of GHGT
doi:10.1016/j.egypro.2013.06.446

viscous than the in-situ brine at the depths it is planned to be emplaced [4]. A potential solution is engineering the CO_2 storage projects in such a way that any potential leaks would be self-sealing.

Our method to prevent leakage from storage sites is inspired by the observation that suitably chemically coated nanoparticles can be used to stabilize CO_2-in-water emulsions [5, 6]. Surface treated nanoparticles adhere to the surface of CO_2 bubbles and prevent their coalescence. However, due to large adhesion energy [5] mechanical work must be applied to bring the nanoparticles from bulk phases to the CO_2 /water interface. Previous observations show that co-injection of CO_2 and nanoparticle suspension at high flow rates (and thus high energy) will produce CO_2/brine foam, while co-injection at low flow rates does not produce foam [5, 7]. In terms of CO_2 storage, foam generation by co-injecting CO_2 and nanoparticle solution may be less than ideal as it reduces the injectivity of the well and discourages other CO_2 trapping mechanisms (capillary and dissolution trapping) from occurring during the course of CO_2 injection. However, as the CO_2 displaces the nanoparticle suspension along a leakage path, the formation of foam will reduce the mobility of the CO_2 and potentially prevent catastrophic leaks [8].

To use this idea for secure sequestration, one could first inject nanoparticles along the leakage path of the prospective storage structure or even into an overlying formation. Therefore, if the buoyant CO_2 were to rise through any of the nanoparticle treated rock, the nanoparticles would be attracted to the CO_2/brine interface and form a CO_2-in-brine foam and eventually seal the leak.

In this work, we investigate the mechanism for this form of leak prevention. We conduct core floods in which CO_2 or a CO_2-analogue fluid displaces brine with and without dispersed nanoparticles. The in-situ saturation distribution of both phases is captured in real time by placing the core horizontally in a modified medical scanner. Pressure transducers were used to measure the pressure gradient during displacement, from which the mobility of the invading phase along the core can be inferred. The proof of concepts describe here offers a new form of passive barrier against CO_2 leakage whether driven by pressure (viscous forces) or by buoyancy. It also suggests a remediation strategy whereby nanoparticle dispersion could be injected into a leakage pathway after CO_2 escape has been discovered.

2. Materials and Method

In this study, we used silica nanoparticles with a nominal diameter of 5 nm, from 3M® (Minneapolis, MN). The nanoparticles were surface-modified with polyethylene-glycol (PEG) ligand. Previous experiments have shown that the PEG-coated nanoparticles stabilized CO_2-in-water foams and *n*-octane-in-water emulsions. The coating also enhanced the transportability of the nanoparticle through the porous media by minimizing its retention in the porous media [9]. The nanoparticles were received as a 19 wt% dispersion which was diluted to 5 or 10 wt% with brine for the total salinity of 2 wt%. Each diluted dispersion was stirred for 30 minutes with a magnetic stirrer to ensure homogeneity of the dispersion.

The core flooding setup was a modified version of the apparatus described in [10, 11]. A schematic diagram of the set-up is shown in Figure 1. The Boise sandstone core sample was wrapped in a heat-shrinkable Teflon tube, 4 layers of aluminum foil, another layer of Teflon shrinking tube, and an AFLAS rubber sleeve, before it was placed in to an aluminum core holder. The Teflon layers provide a barrier to water, while the aluminum foils prevent the leakage of CO_2. The aluminum core holder was used to avoid high-density contrast between the core holder and the rock, which can be detrimental for CT scan measurement [12].

A dual Teledyne Isco pump was used to inject brine and CO_2 continuously to the core through CO_2 and brine accumulators (Figure 2). The accumulators were also used to pre-equilibrate initial and injected fluid before the experiment, by injecting 100 ml of CO_2 per liter of the brine into the brine accumulator, and 10 ml of brine per liter of CO_2 over 5 hours and letting the fluids equilibrate for 40 hours before usage.

Table 1. Viscosity μ, density ρ, interfacial tension with respect to brine σ, and capillary number N_{Ca} at the experiment flux. 5% nano and 10% nano refer to the nanoparticle suspensions in brine that were used. The CO_2 properties are at experimental condition T = 25 °C and P = 1350 psi; all other properties are at room temperature and pressure [14, 15]

	Brine	5% Nano	10% Nano	*n* -octane	CO_2
μ (cP)	1.05	1.2	1.3	0.54	0.075
ρ (kg/m^3)	1010	1040	1080	703	792
σ (mN/m)	N/A	N/A	N/A	51	24
N_{Ca}	N/A	N/A	N/A	4×10^{-8}	2×10^{-7}

In all the experiments, the working porous media were 30 cm long, 7 cm diameter cylindrical Boise sandstone core (porosity 27.5% and permeability about 1 D). High pressure liquid CO_2 or *n*-octane was injected at 0.02 cm/min to displace brine (hereafter called control experiment) or nanoparticle (hereafter called nanoparticle experiment) for approximately 1 PV. *n*-Octane was used as a low pressure analog to high pressure CO_2, as it mimics the key features of CO_2 in the sense that both fluids a) form nanoparticle stabilized droplets, b) have roughly the same density, c) give displacements that are capillary dominated, and d) cause an unstable displacement. The relevant fluid parameters are listed in Table 1.

The in-situ saturation was captured in real time by placing the core horizontally in a Universal Systems HD-350 modified medical scanner. CT scanning measures the local electron density and therefore mass density of the materials occupying each voxel. Since the non-wetting phase is less dense than the brine or nanoparticle suspension (see Table 1) the measured density can be converted to saturation. This can be done by linear interpolation between CT values of the voxel saturated with the wetting phase and non-wetting phase.

The scanning procedure consisted of taking scans every 1 cm along the core. The resolution of the scanner after image filtration (to reduce the noise associated with the image construction [13]) was 1 mm. The core was scanned every 5 minutes for early time during the displacement and every 15 minutes after the invading fluid had broken through.

3. Results

Figure 2a shows lateral CT scans (x-y plane) at different longitudinal (z) positions along the core after injecting 0.10 PV of *n*-octane with brine (2 wt% salinity) as the initial fluid. Images are at equal intervals of 1 cm along the core starting at the distance of 2 cm from the inlet. In these figures full brine saturation is illustrated by red, and *n*-octane is blue. These scans show that the displacement front is not uniform, with regions of high water saturation next to the regions which are mostly saturated with *n*-octane. In particular, going from the inlet towards the center of core, at a distance of 2-3 cm the left hand side of the column is still filled with brine, at a distance of 5-7 cm *n*-octane fingers are seen branching out, and at a distance of 8-9 cm a single finger of *n*-octane is seen in the 4 o'clock position. Within the long *n*-octane

fingers the average brine saturation is roughly $S_w \sim 0.23$ (e.g., see 3 cm position), adjacent to upswept regions have an average brine saturation of $S_w \sim 0.94$ (e.g., see 3 cm position).

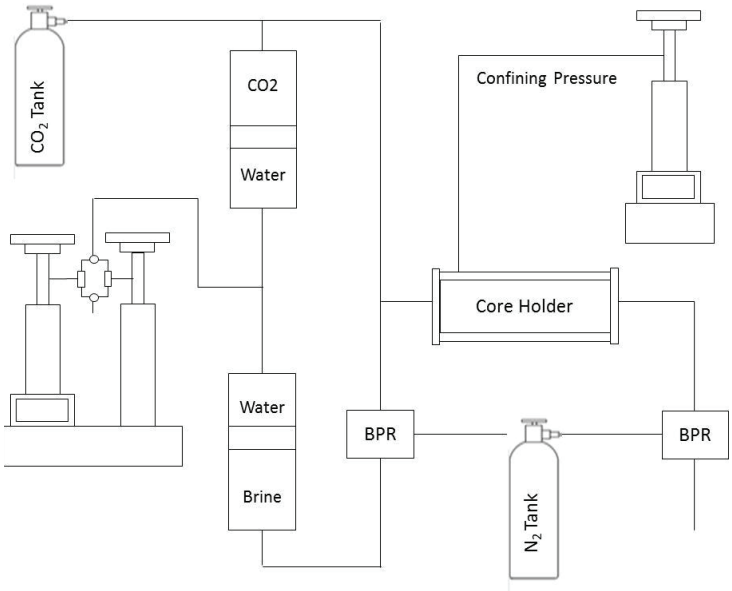

Figure 1: Schematic diagram of the core flooding set-up

Figure 2b shows the saturation profiles at the same time and position as in Figure 2a with 10 wt % nanoparticle suspension as the initial fluid. The core is identical in Figures 2a and 2b. The only difference is the nanoparticle suspension as the initial fluid in Figure 2b, as opposed to the brine in Figure 2a. These scans show a much more distinct and uniform front. Comparing to the control experiment in Figure 2a, these images show much less lateral variations of *n*-octane and thus little or no fingering. Moreover, in the regions behind the front that are most filled with *n*-octane, the water saturation is still rather high at $S_w \approx 0.42$, indicating mixing of water and *n*-octane rather than displacement. Uniform saturation distribution along the core and mixing between water and oil is likely the sign of formation of high viscosity fluid mixture of water and *n*-octane.

Figure 3a shows the side view of the core after injecting 0.25 PV of CO_2 with brine as the initial fluid. This x-z image was obtained by averaging the saturation over the middle 1 cm of the core in the y-direction. The gravity segregation is evident with a leading tongue of CO_2 along the top of the core near the outlet. The heterogeneity can also be observed with a large region of CO_2 between 15 and 20 cm in the longitudinal *x*-direction. As a result of high viscosity ratio ($\mu_{CO2}/\mu_{brine} = 14$), the preferential movement of CO_2 is evident.

Figure 3b shows the saturation distribution at the same time and position as in Figure 3a with nanoparticle suspension as the initial fluid. Because the core is the same, some of the same heterogeneity-dominated flow can be seen in Figure 3b with a large CO_2 region in the lower half between 15 and 20 cm. The effect of nanoparticles can be seen as a) the leading CO_2 tongue ($x > 30$ cm) is not visible in the nanoparticle case and b) the entrance region ($x < 10$ cm) has a higher saturation of CO_2 in the nanoparticle case than the control case. Moreover, the results show wider fingers, leading to a slower front movement, and a higher overall CO_2 saturation behind the front.

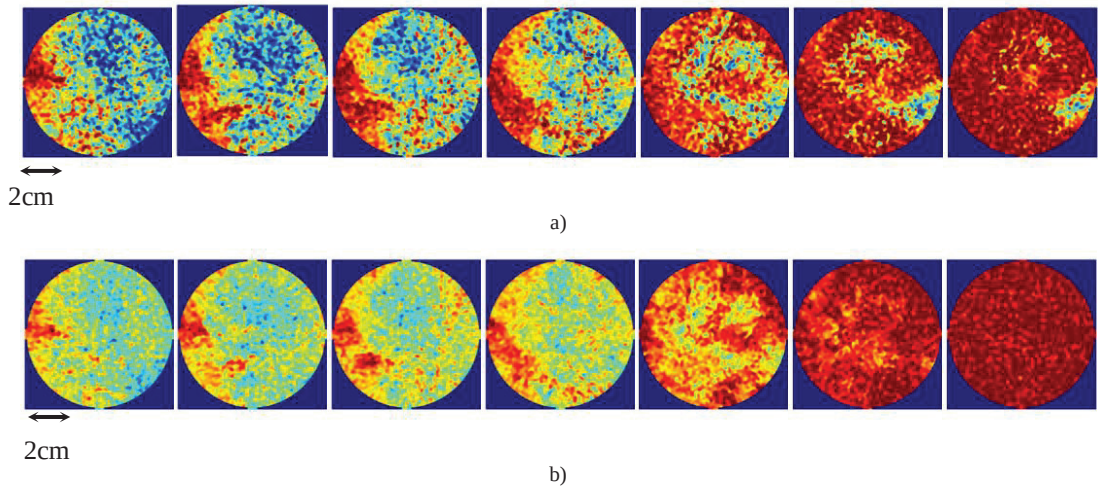

Figure 2. CT scans of water saturation distribution along the core after injecting 0.1 PV *n*-octane. Each slice is 1 cm apart longitudinally. a) Core is initially filled with brine. b) Same core in initially filled with 2% brine containing 10 wt% silica nanoparticles.

Moreover, in order to compare Figure 3a with Figure 3b more quantitatively, the point-by-point difference in CO_2 saturation is shown in Figure 3c. Figure 3c shows different flow pattern in the presence of nanoparticles. The results show more uniform saturation distribution in the presence of nanoparticles, which is also evident in the high permeability region between 15 – 20 cm in x-direction.

In summary, although by adding nanoparticles to the in-situ brine the viscosity ratio and density contrast become more unfavourable, the flow is observed to be more stable with less gravity segregation when compared with the control case.

4. Discussion

The results of the experiments with and without nanoparticles can be summarized as follows:

a) In the presence of nanoparticles, the displacement front becomes stable or self-regulating when *n*-octane was used as the displacing fluid. This is associated with more uniform saturation distribution behind the front, higher pressure drop, and more remaining water saturation.

b) CO_2 displacing nanoparticle-laden brine shows slower displacement front with more uniform CO_2 saturation near the inlet. Moreover, in the presence of nanoparticle the displacement shows less gravity override.

In the classical analysis of fluid displacement, the flow front will be viscously unstable if the viscosity of the invading phase is less than the viscosity of the initial phase. This is the case for both *n*-octane and CO_2 when they displace the nanoparticle-free brine, but not to the same extent. *n*-Octane displacing brine has a viscosity ratio of 2 and the CO_2 displacing brine at the experimental pressure and temperature has a viscosity ratio of 14. As expected, in both displacement experiments without nanoparticles, noticeable viscous fingering can be observed. On the other hand, the flow will become stable if the mobility ratio becomes less than 1, i.e. if the presence of the nanoparticles were enough to

cause the apparent mobility of the invading fluid (be it *n*-octane or CO_2) to become greater than the nanoparticle suspension. To achieve stability for either fluid, the nanoparticles would only have to viscosify *n*-octane by a factor of 2.6 while for the CO_2 the increase in viscosity would have to be a factor of 18. Therefore, stable displacement in the *n*-octane experiment can be interpreted as less than unity viscosity ratio. However, in the CO_2 experiment the nanoparticles reduce the mobility of the CO_2, but not enough to completely stabilize the front.

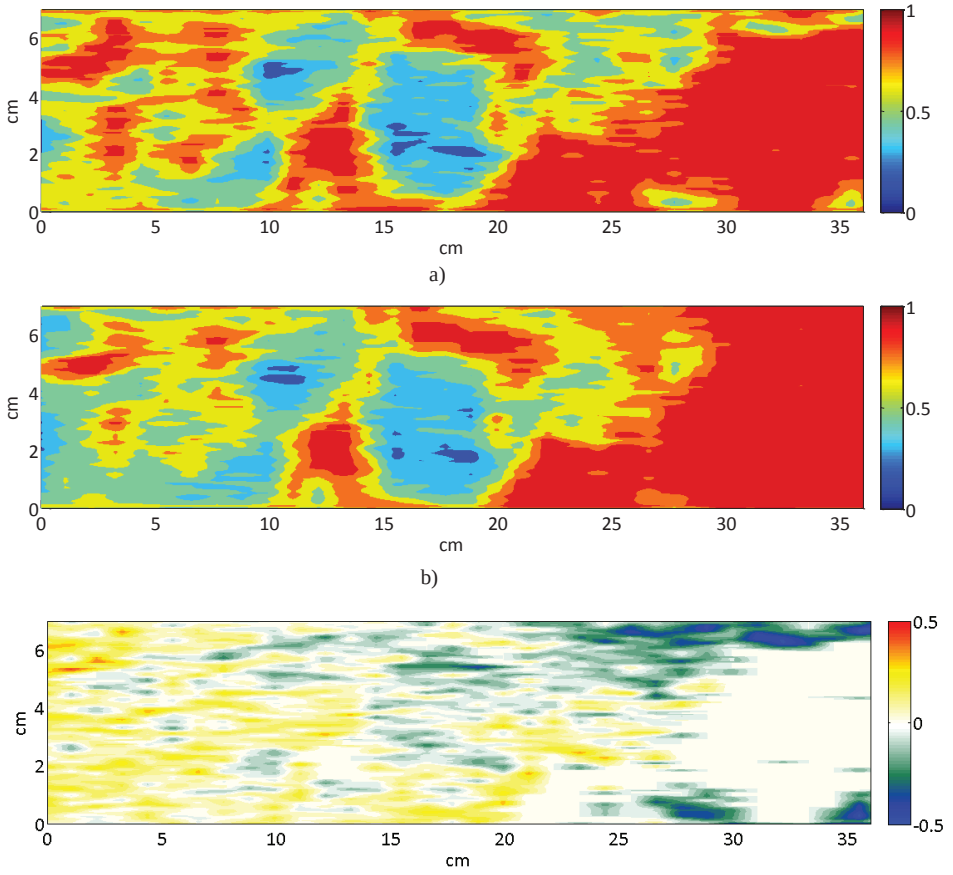

Figure 3. Longitudinal slice through the Boise sandstone core after 0.25 PV of CO_2 injection. a) Initial fluid is 2 wt% brine, b) Initial fluid is 2 wt% brine with 5% silica nanoparticle, and c) the difference between Figure a and b.

There is another subtle difference between CO_2 experiments with and without nanoparticles. Figure 4a shows the CO_2 saturation change over time (in this image, between 0.22 and 0.25 of pore volume of CO_2 injection) with brine as the initial fluid. Classically, it is believed that during a drainage experiment the saturation of wetting phase decreases monotonically with time. However, in this experiment water saturation increased in many regions, including some far upstream of the front. This cannot be due solely to the buoyancy forces, as the increase in water saturation happens at the top part of the core as well as the bottom. Figure 4b shows the CO_2 saturation change between 0.2 and 0.25 PV of CO_2 injection with

5% nanoparticle suspension as the initial fluid. The amount of water imbibition behind the front is less significant in this case.

We propose that this observation has to do with heterogeneity within the core. As CO_2 encounters high-permeability regions inside the core, the capillary pressure required for CO_2 to invade the high-streak region reduced, which ultimately results in a rapid movement of CO_2. This will create a temporary decrease in the local capillary pressure behind the front. This decrease is great enough for the wetting phase to imbibe into the small pores behind the front. On the other hand more uniform saturation distribution in the presence of nanoparticles reduces the capillary pressure drop behind the front, which in turn greatly mitigates this tendency. Moreover, in the presence of nanoparticles CO_2 may be trapped behind the front as the disconnected droplets [8], which discourage the imbibition of water behind the front.

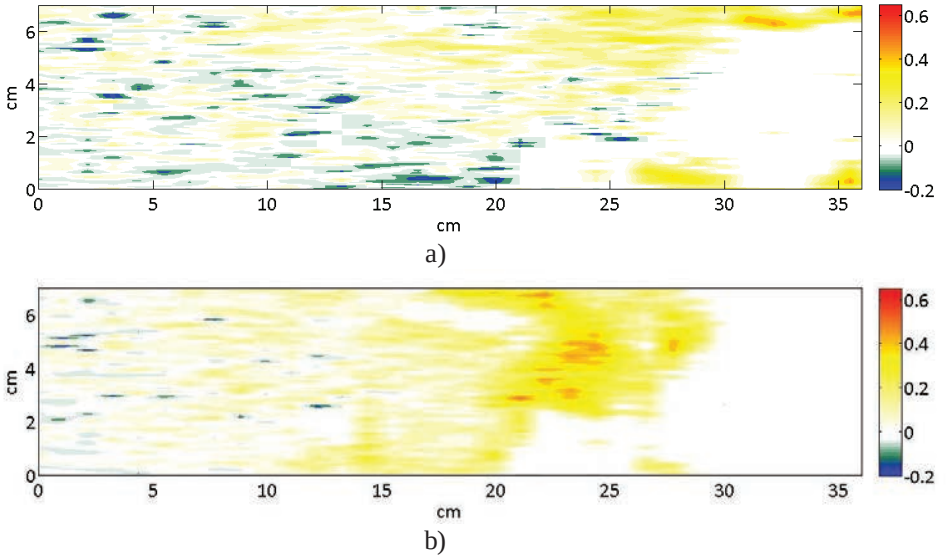

Figure 4. Side view of the CO_2 saturation change between a) 0.22 and 0.25 PV of CO_2 injection with brine as the initial fluid and b) 0.2 and 0.25 PV of CO_2 injection with 5wt% nanoparticle suspension as the initial fluid.

5. Summary and Conclusion

We performed sets of high-pressure liquid CO_2 and CO_2 analogue fluid (*n*-octane) injections into sandstone cores initially filled with brine with and without suspended nanoparticles. When surface treated nanoparticles are in the brine, the propagation of the injected phase displacement front is altered. The alteration increases the sharpness and slows the speed of the front; this behavior is consistent with a reduction of the mobility of the CO_2 or *n*-octane in the presence of nanoparticles. The mechanism appears to be spontaneous generation of nanoparticle-stabilized droplets of the injected phase, which increases the effective viscosity of that phase. Nanoparticles completely stabilized the front when *n*-octane was the injected fluid. Because the CO_2 viscosity is so much smaller than the *n*-octane viscosity, the same particles altered but did not completely stabilize the liquid CO_2 displacement front.

The results suggest that pre-positioning a dispersion of nanoparticles above or within potential leakage paths (e.g. fractures, faults, and abandoned wells) would enable CO_2/brine foam to form if CO_2 enters the path. This could slow or even prevent the leak.

Acknowledgements

This work was supported by the Center for Frontiers of Subsurface Energy Security (CFSES), an Energy Frontier Research Center funded by the U.S. Department of Energy, Office of Science, Office of Basic Energy Sciences under Award Number DE-SC0001114. We are grateful to Dr Jim Baran for providing the nanoparticles used in this work.

References

[1] K. S. Lackner, "A Guide to CO_2 Sequestration," *Science*, vol. 300, pp. 1677-1678, 2003.
[2] IPCC, "Underground Geological Storage. In: Metz B, Davidson O, de Coninck HC, Loos M, Meyer LA (eds) IPCC Special Report on Carbon Dioxide Capture and Storage, prepared by Working Group III of the Intergovernmental Panel on Climate Change.," Cambridge University Press, Cambridge, UK, and New York, USA, 2005.
[3] D. A. DiCarlo, B. Aminzadeh, M. Roberts, D. Chung, S. L. Bryant and C. Huh, "Mobility Control Through Spontaneous Formation of Nanoparticle Stabilized Emulsions," *Geophys. Res. Lett., 38, L24404, doi:10.1029/2011GL050147,* 2011.
[4] R. W. Klusman, "Evaluation of Leakage Potential from a Carbon Dioxide EOR/Sequestration Project," *Energy Conversion & Managment,* vol. 44, pp. 1921-1940, 2003.
[5] D. Espinosa, F. Caldelas, K. Johnston, S. L. Bryant and C. Huh, "Nanoparticle-Stabilized Supercritical CO_2 Foams for Potential Mobility Control Applications," in *SPE paper 129925, Presented at the Improved Oil Recovery Symposium*, 24 - 28 April, Tulsa, OK, 2010.
[6] T. Zhang, A. Davidson, S. L. Bryant and C. Huh, "Nanoparticle-Stabilized Emulsions for Applications in Enhanced Oil Recovery," in *SPE paper 129885, Presented at the Improved Oil Recovery Symposium*, 24 - 28 April, Tulsa, OK, 2010.
[7] A. Worthen, H. G. Bagaria, Y. Chen, S. L. Bryant, C. Huh and K. P. Johnston, "Nanoparticle-Stabilized Carbon Dioxide-in-Water Foams with Fine Texture," *Journal of Colloid and Interface Science,* p. In Press, 2012.
[8] D. A. DiCarlo, B. Aminzadeh, M. Roberts, D. Chung, S. L. Bryant and C. Huh, "Mobility Control Through Spontaneous Formation of Nanoparticle Stabilized Emulsions," *Geophys. Res. Lett., 38, L24404, doi:10.1029/2011GL050147,* 2011.
[9] M. R. Roberts, B. Aminzadeh, D. A. DiCarlo, S. L. Bryant and C. Huh, "Generation of Nanoparticle-Stabilized Emulsions in Fractures," in *SPE paper 154228, Presented at the Improved Oil Recovery Symposium*, 14 - 18 April, Tulsa, OK.
[10] B. Aminzadeh, D. Chung, A. Kianinejad, D. A. DiCarlo, S. L. Bryant and C. Huh, "Effect of Nanoparticles on Flow Alteration During CO_2 Injection," in *SPE paper 154248, Presented at SPE ATCE*, 8 - 10 October, San Antonio, TX, 2012.
[11] B. Aminzadeh, D. A. DiCarlo, M. Roberts, D. H. Chung, S. L. Bryant and C. Huh, "Effect of Spontaneous Formation of Nanoparticle Stabilized Emulsion on the Stability of a Displacement," in *SPE paper 154248, Presented at the Improved Oil Recovery Symposium, 14 - 18 April, Tulsa, OK, 2012.*, 2012.
[12] A. C. Kak and M. Slaney, Principle of Computerized Tompgraphic Imaging, New York: IEEE, 1988.
[13] R. Pini, S. Krevor and S. Benson, "Capillary pressure and heterogeneity for the CO_2/water system in sandstone rocks at reservoir conditions," *Advances in Water Resources,* vol. 38, pp. 48-59, 2012.
[14] N. Vargaftik, Tables of the Thermophysical Properties of Liquid and Gases, Second ed., Hemisphere Publishing Corporation., 2005.
[15] D. A. DiCarlo, A. Sahni and M. Blunt, "Three-phase Relative Permeability of Water-wet, Oil-wet, and Mixed-wet Sandpacks," *SPEJ,* vol. 5, no. 1, pp. 82-91, 2000.